

# UC San Diego

## UC San Diego Previously Published Works

### Title

A tetra(ethylene glycol) derivative of benzothiazole aniline ameliorates dendritic spine density and cognitive function in a mouse model of Alzheimer's disease

### Permalink

<https://escholarship.org/uc/item/6p46872v>

### Authors

Song, Jung Min  
DiBattista, Amanda Marie  
Sung, You Me  
et al.

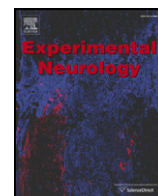
### Publication Date

2014-02-01

### DOI

10.1016/j.expneurol.2013.11.023

Peer reviewed



# A tetra(ethylene glycol) derivative of benzothiazole aniline ameliorates dendritic spine density and cognitive function in a mouse model of Alzheimer's disease

Jung Min Song<sup>a,1</sup>, Amanda Marie DiBattista<sup>a,1</sup>, You Me Sung<sup>g</sup>, Joo Myung Ahn<sup>a</sup>, R. Scott Turner<sup>b</sup>, Jerry Yang<sup>e</sup>, Daniel T.S. Pak<sup>c</sup>, Hey-Kyoung Lee<sup>d,f</sup>, Hyang-Sook Hoe<sup>a,b,\*</sup>

<sup>a</sup> Department of Neuroscience, Georgetown University Medical Center, Washington, DC 20057, USA

<sup>b</sup> Department of Neurology, Georgetown University Medical Center, Washington, DC 20057, USA

<sup>c</sup> Department of Pharmacology, Georgetown University Medical Center, Washington, DC 20057, USA

<sup>d</sup> Department of Neuroscience, Johns Hopkins University, Baltimore, MD 21218, USA

<sup>e</sup> Department of Chemistry and Biochemistry, University of California, San Diego, La Jolla, CA 92093, USA

<sup>f</sup> Department of Bioengineering, University of California, San Diego, La Jolla, CA 92093, USA

<sup>g</sup> College of Pharmacy, Seoul National University, South Korea

## ARTICLE INFO

### Article history:

Received 14 June 2013

Revised 25 October 2013

Accepted 22 November 2013

Available online 6 December 2013

### Keywords:

BTA-EG<sub>4</sub>

Dendritic spine

Ras signaling

3xTg AD mice

## ABSTRACT

We recently reported that the tetra(ethylene glycol) derivative of benzothiazole aniline, BTA-EG<sub>4</sub>, acts as an amyloid-binding small molecule that promotes dendritic spine density and cognitive function in wild-type mice. This raised the possibility that BTA-EG<sub>4</sub> may benefit the functional decline seen in Alzheimer's disease (AD). In the present study, we directly tested whether BTA-EG<sub>4</sub> improves dendritic spine density and cognitive function in a well-established mouse model of AD carrying mutations in APP, PS1 and tau (APP<sup>SWE</sup>;PS1<sup>M146V</sup>;tau<sup>P301L</sup>, 3xTg AD mice). We found that daily injections of BTA-EG<sub>4</sub> for 2 weeks improved dendritic spine density and cognitive function of 3xTg AD mice in an age-dependent manner. Specifically, BTA-EG<sub>4</sub> promoted both dendritic spine density and morphology alterations in cortical layers II/III and in the hippocampus at 6–10 months of age compared to vehicle-injected mice. However, at 13–16 months of age, only cortical spine density was improved without changes in spine morphology. The changes in dendritic spine density correlated with Ras activity, such that 6–10 month old BTA-EG<sub>4</sub> injected 3xTg AD mice had increased Ras activity in the cortex and hippocampus, while 13–16 month old mice only trended toward an increase in Ras activity in the cortex. Finally, BTA-EG<sub>4</sub> injected 3xTg AD mice at 6–10 months of age showed improved learning and memory; however, only minimal improvement was observed at 13–16 months of age. This behavioral improvement corresponds to a decrease in soluble A $\beta$  40 levels. Taken together, these findings suggest that BTA-EG<sub>4</sub> may be beneficial in ameliorating the synaptic loss seen in early AD.

© 2013 Published by Elsevier Inc.

## Introduction

Alzheimer's disease (AD) is a neurodegenerative disease associated with amyloid- $\beta$  (A $\beta$ ) pathology in the brain that contributes to synaptic loss by interacting with cellular components in harmful ways (Finder and Glockshuber, 2007; Habib et al., 2010; Lustbader et al., 2004). Excitatory synapse number is directly correlated with the number of excitatory sites of neurotransmission known as dendritic spines.

Dendritic spines act as sites of learning and memory in the brain. Transient thin spines are thought to represent molecular sites of learning, while the persistent wider spines may represent molecular sites of memory (Kasai et al., 2002; Yasumatsu et al., 2008). Additionally, age-dependent synapse loss is common to many transgenic mouse models of AD, including 3xTg AD mice (Knobloch and Mansuy, 2008). Interestingly, several studies have indicated that dendritic spine loss may be correlated with cognitive impairment more strongly than A $\beta$  plaque levels in AD (Knobloch and Mansuy, 2008; Masliah et al., 2006; Scheff and Price, 2006; Scheff et al., 2006; Selkoe, 2002; Terry et al., 1991). For instance, dendritic spine density is reduced in hippocampal region CA1 in patients with a diagnosis of early Alzheimer's disease (Scheff et al., 2007). Moreover, synapse number correlates with Mini Mental Status Exam (MMSE) score in layer III of the frontal cortex in human AD patients (Scheff and Price, 2006). Thus, measurement of dendritic

Abbreviations: AD, Alzheimer's disease; A $\beta$ , amyloid- $\beta$ .

\* Corresponding author at: Convergence Brain Research Department, Korea Brain Research Institute (KBRI), 425, Jungang-daero, Jung-gu, Daegu 700-010, South Korea, Department of Neurology, Department of Neuroscience, Georgetown University, 3970 Reservoir Road, NW, Washington, DC 20057-1464, USA. Fax: +82 53 428 1851.

E-mail address: [sookhoe72@kbri.re.kr](mailto:sookhoe72@kbri.re.kr) (H.-S. Hoe).

<sup>1</sup> JMS and AMD contributed equally to this work.

spine morphology and density is used here to quantify synapse loss in the CA1 region of the hippocampus and cortical layers II/III in 3xTg AD mice.

Our previous research has demonstrated that members of the benzothiazole aniline (BTA) class of compounds directly interact with A $\beta$  and can prevent A $\beta$ -induced cytotoxicity (Capule and Yang, 2012; Habib et al., 2010; Inbar et al., 2006). Additionally, we found that a tetra-ethylene glycol derivative of BTA (BTA-EG<sub>4</sub>) can penetrate the blood–brain barrier and has no toxicity (Capule and Yang, 2012; Inbar et al., 2006). Moreover, our recent work demonstrated that BTA-EG<sub>4</sub> alters normal synaptic function *in vitro* and *in vivo* by acting through amyloid precursor protein (APP) to target Ras-dependent spinogenesis (Megill et al., 2013). This increase in dendritic spine density and the number of functional synapses, as observed by elevated frequency of AMPA-receptor-mediated miniature excitatory postsynaptic currents (mEPSCs), was accompanied by improved memory in cognitive tasks (Megill et al., 2013).

In the present study, we examined whether BTA-EG<sub>4</sub> can improve synapse loss and cognitive deficits in a mouse model of AD. We report here that BTA-EG<sub>4</sub>-injected 3xTg AD mice demonstrate age-specific improvements in dendritic spine density and morphology in cortical layers II/III and the CA1 region of the hippocampus. We also found that Ras activity correlated with the age-dependent increase in dendritic spine density following BTA-EG<sub>4</sub> treatment. Moreover, at 6–10 months BTA-EG<sub>4</sub> substantially improved, while at 13–16 months BTA-EG<sub>4</sub> modestly improved, learning and memory after daily injection for 2 weeks. These results suggest that BTA-EG<sub>4</sub> warrants further investigation with a longer duration of treatment as a novel therapeutic option for AD patients to mitigate synaptic loss and cognitive impairment.

## Materials and methods

### Synthesis of 2-(2-(2-(2-hydroxyethoxy)ethoxy)ethoxy)ethyl toluenesulfonate

Tetra-ethylene glycol (10.0 g, 51.5 mmol) was dissolved with a stir bar in a clean, dry 1 L round bottom flask using 500 mL dry dichloromethane (DCM) at room temperature. The following were successively added to the reaction flask after 5 min: potassium iodide (1.71 g, 10.3 mmol), Ag<sub>2</sub>O (17.9 g, 77.2 mmol), and *p*-toluenesulfonyl chloride (10.8 g, 56.6 mmol). After 2 h of vigorous stirring, the reaction mixture was filtered through celite and concentrated *in vacuo* after solids were removed. Silica column chromatography (100% DCM to 95:5 DCM:CH<sub>3</sub>OH) was used to purify the residue to produce 2-(2-(2-(2-hydroxyethoxy)ethoxy)ethoxy)ethyl toluenesulfonate as a colorless oil (13.2 g, 74%). <sup>1</sup>H NMR (400 MHz, CDCl<sub>3</sub>):  $\delta$  = 7.74 (d, 8.0 Hz, 2H), 7.30 (d, 8.0 Hz, 2H), 4.11 (t, 4.8 Hz, 2H), 3.66–3.53 (m, 12H), 2.79 (s, 1H), 2.39 (s, 3H). <sup>13</sup>C NMR (100 MHz, CDCl<sub>3</sub>):  $\delta$  = 145.04, 133.17, 130.10 (2C), 128.19 (2C), 70.95, 70.79, 70.70, 69.49, 68.88, 21.87. ESI-MS (*m/z*) calculated for C<sub>15</sub>H<sub>24</sub>O<sub>7</sub>S [M]<sup>+</sup> 348.1243; found [M + H]<sup>+</sup> 348.96, [M + NH<sub>4</sub>]<sup>+</sup> 365.94 and [M + Na]<sup>+</sup> 371.08.

### Synthesis of 2-(2-(2-(2-iodoethoxy)ethoxy)ethoxy)ethanol

In a clean, dry round bottom flask, 2-(2-(2-(2-hydroxyethoxy)ethoxy)ethoxy)ethyl toluenesulfonate (12.01 g, 34.5 mmol), sodium iodide (20.7 g, 137.9 mmol) and 200 mL dry acetone were heated to reflux with vigorous stirring. Twelve hours later, the reaction was diluted with 100 mL ethyl acetate after cooling to room temperature. 2-(2-(2-(2-iodoethoxy)ethoxy)ethoxy)ethanol as a pale yellow oil (5.61 g, 54%) was attained by washing the organic phase with 10% Na<sub>2</sub>S<sub>2</sub>O<sub>3</sub> (2  $\times$  10 mL), deionized H<sub>2</sub>O (1  $\times$  20 mL), saturated NaCl (1  $\times$  20 mL), followed by drying over anhydrous Na<sub>2</sub>SO<sub>4</sub>, filtering, and *in vacuo* concentration. <sup>1</sup>H NMR (400 MHz, CDCl<sub>3</sub>):  $\delta$  = 3.73–3.58 (m, 14H), 3.24 (t, 2H), 2.59 (s, 1H). <sup>13</sup>C NMR

(100 MHz, CDCl<sub>3</sub>):  $\delta$  = 72.70, 72.19, 70.90, 70.76, 70.58, 70.39, 61.94, 3.07.

### Synthesis of BTA-EG<sub>4</sub>

A microwave reaction tube was equipped with a small stir bar, sealed and placed in a microwave reactor (125 °C for 2 h) following charging with 2-(2-(2-(2-iodoethoxy)ethoxy)ethoxy)ethanol (1.47 g, 4.83 mmol), benzothiazole aniline (3.49 g, 14.5 mmol), potassium carbonate (3.34 g, 24.2 mmol) and 20 mL dry THF. The reaction was filtered to remove solids after cooling to room temperature, and solids were washed with DCM several times until the filtrate was colorless. The desired BTA-EG<sub>4</sub> compound as a yellow solid (1.13 g, 56%) was given after the combined organic layers were concentrated *in vacuo* and purified by column chromatography. <sup>1</sup>H NMR (400 MHz, CDCl<sub>3</sub>):  $\delta$  = 7.87 (d, 8.8 Hz, 2H), 7.83 (d, 8.4 Hz, 1H), 7.63 (s, 1H), 7.23 (d, 8.4 Hz, 1H), 6.68 (d, 8.8 Hz, 2H), 3.76–3.64 (m, 14H), 3.37 (t, 5.2 Hz, 2H), 2.47 (s, 3H). <sup>13</sup>C NMR (100 MHz, CDCl<sub>3</sub>):  $\delta$  = 168.03, 152.64, 150.92, 134.87, 134.47, 129.13 (2C), 127.70, 122.88, 122.03, 121.41, 112.82 (2C), 72.86, 70.88, 70.69, 70.43 (2C), 69.64, 61.91, 43.32, 21.70. HR-ESI-MS (*m/z*) calculated for C<sub>22</sub>H<sub>28</sub>N<sub>2</sub>O<sub>4</sub>SNa [M + Na]<sup>+</sup> 439.1662; found [M + Na]<sup>+</sup> 439.1660.

### Animals

Male homozygous 3xTg AD mice were generated from mutant PS-1 (M146V) knock-in mice by microinjection of the following transgenes under the control of the Thy 1.2 promoter: human APP (K670M/N671L) and tau (P301L) on a hybrid 129/C57BL6 background (Oddo et al., 2003). All animal maintenance protocols and experiments were approved by the Institutional Animal Care and Use Committee at Georgetown University.

### Golgi staining and morphological analysis of dendritic spines

Dendritic spine density and morphology analyses in the brain were conducted using the FD Rapid GolgiStain Kit (FD NeuroTechnologies, Ellicott City, MD, USA). Mouse brains were dissected, immersed in Solutions A and B (2 weeks, room temperature, dark conditions), and then transferred to Solution C (24 h, 4 °C). A VT1000S Vibratome (Leica, Bannockburn, IL, USA) was then used to slice brains 150  $\mu$ m thick. Bright-field microscopy acquired dendritic images by Axioplan 2 (Zeiss, Oberkochen, Germany). Scion image software (Scion Corporation, Frederick, MD, USA) allowed measurement of spine head width, spine length, and linear density of cortical layers II/III and CA1 of the hippocampus. Images were coded and analyzed blind to experimental conditions. To measure dendritic spine density, we included spines from 0.2 to 2  $\mu$ m in length, with at least 25 apical oblique (AO) and basal (BS) dendritic observations averaged from each animal (*n* = 4–5 brains for 2–3 months old/group and 6–10 months old/group, *n* = 3 brains for 13–16 months old/group). To measure spine morphology, we included spines up to 1.4  $\mu$ m in width and 3.2  $\mu$ m in length.

### Ras activity assay

Brain lysate from 3xTg AD mice at 6–10 months or 13–16 months of age was homogenized with Ral buffer (25 mM Tris–HCl, pH 7.4, 250 mM NaCl, 0.5% NP40, 1.25 mM MgCl<sub>2</sub>, and 5% glycerol) to measure active Ras levels. Briefly, brain lysate was incubated with GST-Raf-RBD purified protein coupled with glutathione sepharose (Amersham) overnight at 4 °C. After 24 h, pellets were washed with Ral buffer and western blotting was conducted with anti-Ras.

## Western blot and analysis

3xTg AD mice were injected with 30 mg/kg BTA-EG<sub>4</sub> or vehicle daily for 2 weeks. After 2 weeks, the cortex and hippocampus were dissected and homogenized with RIPA buffer. Brain lysates were reduced, boiled, and run on a polyacrylamide gel followed by transfer onto nitrocellulose membrane and incubation in the following primary antibodies: rabbit anti-RasGRF1 (Santa Cruz, C-20), rabbit anti-GluA1 (Millipore, ab1504), mouse anti-GluA2 (Neuromab), rabbit anti-p-ERK (Invitrogen, 36880), or p-Elk (Cell Signal, 9181). Primary antibodies were applied overnight, washed with TBS buffer (3 washes, 5 min each), and HRP-conjugated secondary antibodies were applied for 1 h. After 1 h, membranes were washed with TBS buffer (3 washes, 5 min each) and proteins were visualized by affixing the blots to autoradiography film. The density of each band was then quantified using ImageJ software as a percentage of control following normalization to  $\beta$ -actin.

## Morris Water Maze

To examine the effects of BTA-EG<sub>4</sub> on learning and memory, we injected 2–3 month old, 6–10 month old, and 13–16 month old 3xTg AD mice daily (i.p.) for 2 weeks before beginning behavioral testing as described previously (Minami et al., 2012). The control group was treated with vehicle solution (1% DMSO) while the experimental group was treated with BTA-EG<sub>4</sub> (30 mg/kg) daily for 2 weeks. Animals were kept on a fixed 12 hour light–dark cycle, and behavioral experiments were conducted during the light portion of this cycle. Specifically, experiments began at 9:30 AM and concluded before 4:00 PM. Briefly, the amount of time required for animals to locate a Plexiglas platform submerged in opaque water was measured in a large circular pool. The animal was randomly placed into one of four quadrants separated by 90°, and the platform was hidden in one of these quadrants (14 in. from the wall). TOPSCAN software tracked the time required (latency, limited to 60 s) to locate the hidden platform, and animals failing to locate the platform within 60 s were gently guided to the platform. On the first trial, animals were allowed to remain on the platform for 15 s. All subsequent trials limited platform time to 10 s, and a probe trial (60 s) was administered 24 h after the final learning trial. Time spent in the quadrant where the platform was previously located and number of platform crossings were recorded during this probe trial. As a control, 12 h after the last trial, animals were required to locate a clearly visible black platform placed in a new location.

## Statistical analyses

All data were analyzed using either a 2-tailed *t*-test or 1-way ANOVA with Tukey's Multiple Comparison test for post-hoc analyses (Graphpad Prism 4 software, GraphPad, La Jolla, CA). Significance was determined as  $p < 0.05$ . To analyze the Morris Water Maze escape latencies during the training phase, we used 2-way ANOVA with Tukey's Multiple Comparison test for post-hoc analyses. Descriptive statistics were calculated with StatView 4.1 and expressed as mean  $\pm$  SEM.

## Results

### BTA-EG<sub>4</sub> alters dendritic spine density in the cortex and hippocampus

We recently reported that BTA-EG<sub>4</sub>-injected wild-type mice exhibited increased dendritic spine density in the cortex and hippocampus (Megill et al., 2013). In the present study, we investigated whether BTA-EG<sub>4</sub> improves dendritic spine density in a mouse model of AD. For this study, we selected the 3xTg AD mouse model due to its ability to model the progression of human AD (Oddo et al., 2003). This AD mouse model exhibits mild synapse loss at 6–10 months of age, and moderate loss by 13–16 months. To assess its effectiveness throughout disease progression, 2–3 month, 6–10 month, and 13–16 month old

3xTg AD mice were injected with BTA-EG<sub>4</sub> (30 mg/kg, i.p.) or vehicle (1% DMSO) daily for 2 weeks. The 2-week duration of treatment was selected because it increased dendritic spine density and improved memory in wild-type mice (Megill et al., 2013). After the treatment, we conducted Golgi staining to measure dendritic spine density (Fig. 1, Supplementary Figs. 1 and 2). We found that BTA-EG<sub>4</sub> injection significantly increased the overall density of dendritic spines in both the layers II/III of the cortex and the hippocampus CA1 at 2–3 months ( $n = 4$ –5 brains/group) and 6–10 months of age ( $n = 4$ –5 brains/group), but only improved the dendritic spine density of cortical neurons at 13–16 months of age (Fig. 1, Supplementary Figs. 1 and 2,  $n = 3$  brains/group). There were subtle differences in the effect of BTA-EG<sub>4</sub> on dendritic spine density of apical oblique (AO) and basal (BS) dendrites at different ages, but overall our data suggest that the effectiveness of BTA-EG<sub>4</sub> in improving dendritic spine density is reduced in older 3xTg AD mice.

### BTA-EG<sub>4</sub>-injected 3xTg AD mice had wider and longer dendritic spines at 6–10 months old

Next, we further analyzed whether BTA-EG<sub>4</sub> could regulate dendritic spine morphology by measuring spine head width and spine length in cortical layers II/III and hippocampal region CA1. We found that 6–10 month old 3xTg AD mice injected with BTA-EG<sub>4</sub> (30 mg/kg) had wider dendritic spines compared to vehicle-injected mice in the cortex and hippocampus using cumulative distribution analysis (Figs. 2A, C) as well as comparison of average dendritic spine width (Figs. 2I, K,  $n = 4$ –5 brains/group). Additionally, 6–10 month old BTA-EG<sub>4</sub> injected 3xTg AD mice also had longer dendritic spines in cortical layers II/III and hippocampus (Figs. 2B, D, J, L,  $n = 4$ –5 brains/group). However, neither the width nor length of dendritic spines changed when BTA-EG<sub>4</sub> was administered to 13–16 month old 3xTg AD mice (Figs. 2E–H, 2I–L,  $n = 3$  brains/group). Taken together, these data suggest that BTA-EG<sub>4</sub> treatment promotes dendritic spine density and alters dendritic spine morphology in cortical layers II/III and the CA1 region of the hippocampus of 3xTg AD mice at 6–10 months of age, which is before severe A $\beta$  plaque deposition and synapse loss.

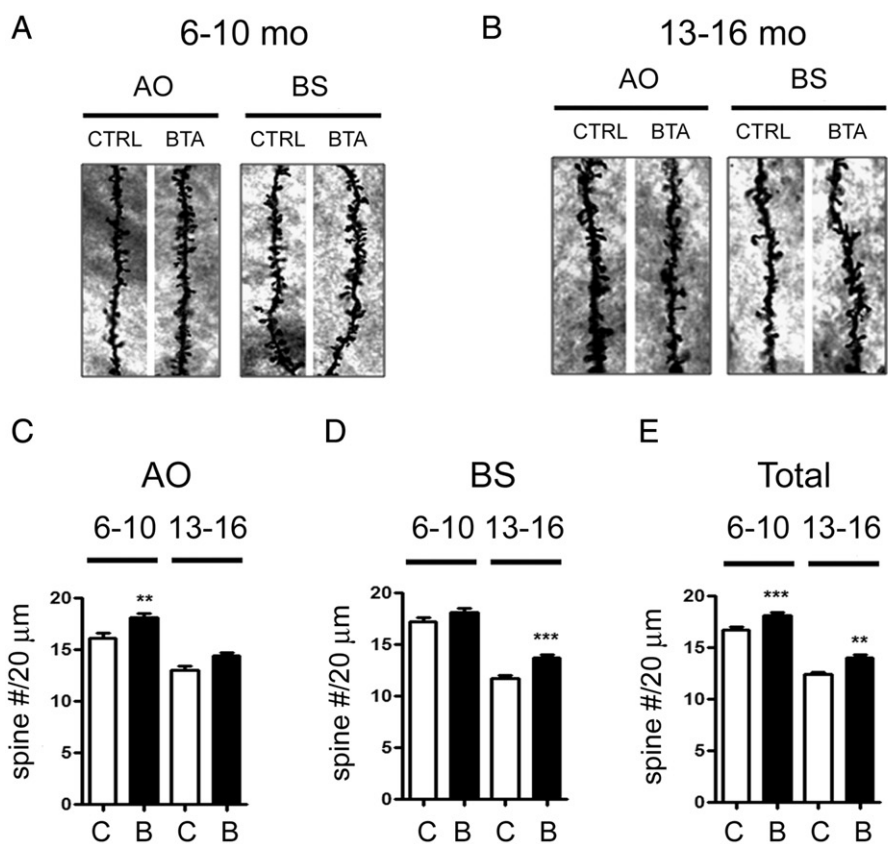
### BTA-EG<sub>4</sub> injected 6–10 month old 3xTg AD mice had increased Ras activity

Our recent study demonstrated that BTA-EG<sub>4</sub> promoted dendritic spine density in a Ras-dependent manner in wild-type mice (Megill et al., 2013). Therefore, we examined whether the same mechanism is shared for improving dendritic spine density in the 3xTg AD mouse model. To test this, 6–10 month old or 13–16 month old 3xTg AD mice were injected with 30 mg/kg BTA-EG<sub>4</sub> or vehicle daily for two weeks. After two weeks, mouse brains were homogenized with Ral buffer and levels of active Ras and RasGRF1 (a Ras effector) were measured via Western blot. We found that Ras activity was increased in the cortex and hippocampus of 6–10 month old BTA-EG<sub>4</sub>-injected 3xTg AD mice (Figs. 3A–D,  $n = 2$  brains/group). However, Ras activity was unchanged in the cortex and hippocampus of 13–16 month old mice (Figs. 3E–H,  $n = 2$  brains/group). Ras activity changes with BTA-EG<sub>4</sub> were corroborated by similar age specific increases in the level of RasGRF1 (Figs. 3I–Q,  $n = 3$ –4 brains/group). These data suggest that BTA-EG<sub>4</sub> may promote dendritic spine density in 3xTg AD mice by modulating the Ras activity.

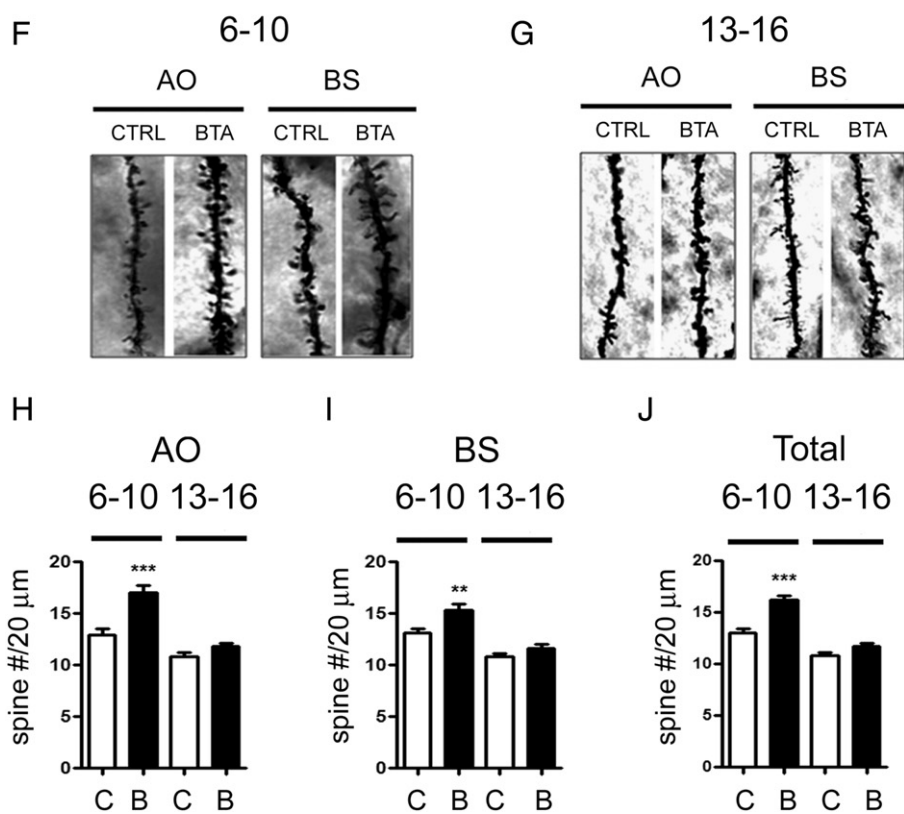
### BTA-EG<sub>4</sub> injected 3xTg AD mice had increased GluA2 levels

Next, we investigated whether BTA-EG<sub>4</sub> could alter downstream targets of the Ras signaling pathway. To test this, 6–10 month or 13–16 month old 3xTg AD mouse brains were homogenized following BTA-EG<sub>4</sub> (30 mg/kg) or vehicle injection daily for 2 weeks. Using Western blots with specific GluA1 and GluA2 antibodies, we found an age-specific increase in the GluA2 subunit of AMPA receptors

## Cortical layers II/III



## Hippocampus



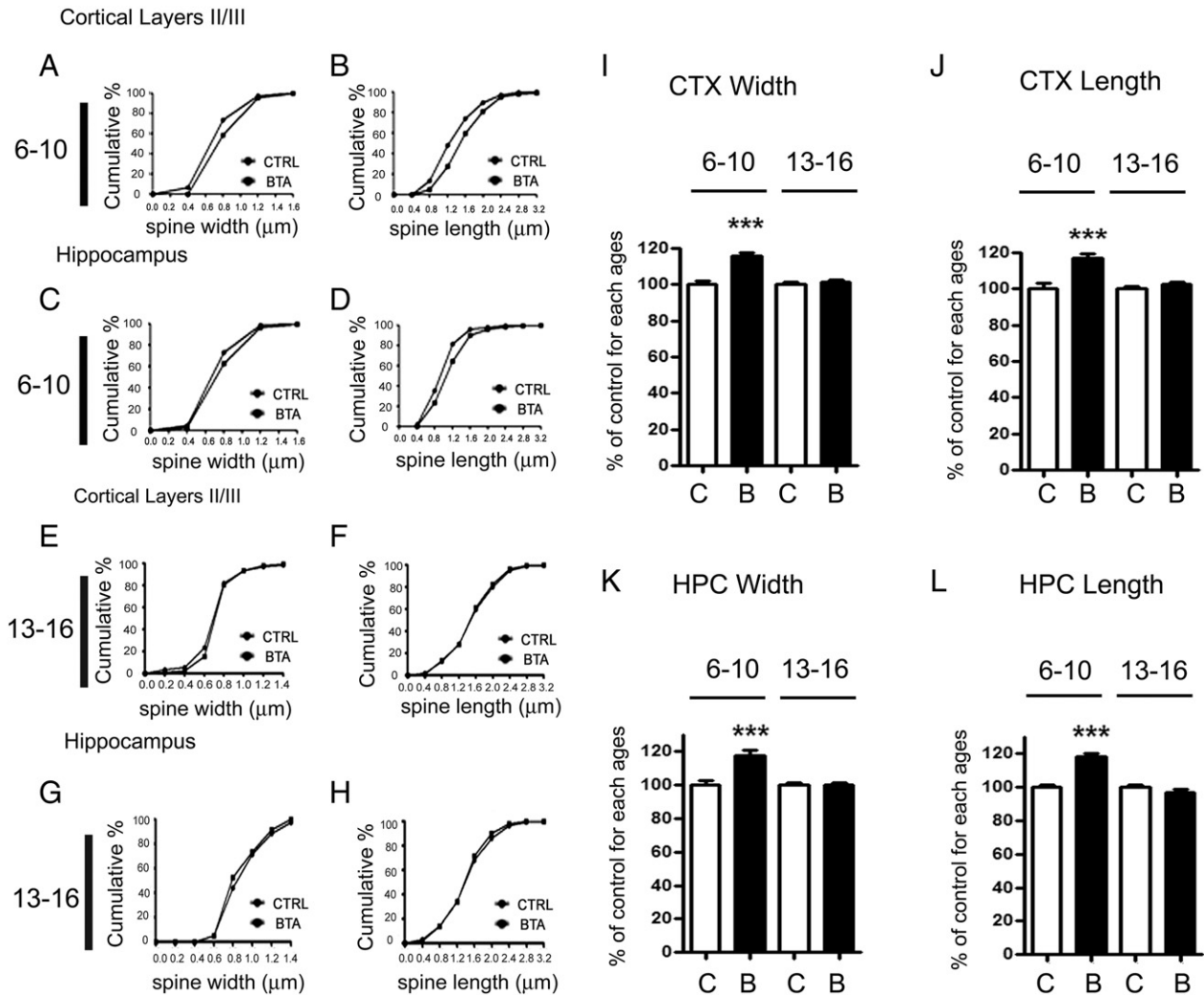


**Fig. 2.** BTA-EG<sub>4</sub> alters dendritic spine morphology in 6–10 month-old, but not 13–16 month old, 3xTg AD mice. (A–D) Dendritic spine morphology as a cumulative distribution plot of spine head width (A,C) and spine length (B,D) in cortical layers II/III (A–B) and hippocampal region CA1 (C–D) in 6–10 month old mice treated with BTA-EG<sub>4</sub> (Kolmogorov–Smirnov test,  $n = 4–5$  brains/group; \* $p < 0.05$ ). (E–H) Dendritic spine morphology as a cumulative distribution plot of spine head width (E,G) and spine length (F,H) in cortical layers II/III (E–F) and hippocampal region CA1 (G–H) at 13–16 month old mice treated with BTA-EG<sub>4</sub> (Kolmogorov–Smirnov test,  $n = 3$  brains/group). (I–L) Summary of the average width of dendritic spines in the cortex (I) and hippocampal CA1 region (K) following BTA-EG<sub>4</sub> treatment as a percentage of control levels for each age. Summary of the averaged dendritic spine lengths in the cortex (J) and hippocampal CA3 (L) following BTA-EG<sub>4</sub> (“B”) or control (“C”) treatment for 2 weeks a percentage of control levels for each age. \*\*\* $p < 0.001$ .

with BTA-EG<sub>4</sub> treatment. Specifically, GluA2 levels were increased in 6–10 month old 3xTg AD mouse hippocampus without a significant change in the GluA1 levels (Figs. 4C–D,  $n = 3–4$  brains/group). There was only a trend of an increase in GluA2 in the cortex (Figs. 4A–B,  $n = 3–4$  brains/group). In the older 3xTg AD mice (13–16 months old), there was no statistically significant change in the levels of AMPA receptor subunits in either brain area (Figs. 4E–H,  $n = 3–4$  brains/group). We then examined whether BTA-EG<sub>4</sub> injection could also alter the levels of p-ERK and ERK in 3xTg AD mice. To test this, 6–10 month old or 13–16 month old 3xTg AD mice were injected with 30 mg/kg BTA-EG<sub>4</sub> or vehicle daily for two weeks prior to measuring the levels of p-ERK and ERK. Unexpectedly, we found that BTA-EG<sub>4</sub> injected 6–10 month old 3xTg AD mice did not have altered levels of p-ERK and ERK in the cortex and hippocampus (Supplementary Figs. 3A–F). Moreover, we found that BTA-EG<sub>4</sub> injection in 6–10 month old 3xTg AD mice or 13–16 month old 3xTg AD mice did not alter the

levels of p-Elk, which is a downstream target of phosphorylated ERK (Supplementary Figs. 3G–H). Hence, the increases in AMPA receptor subunit GluA2 expression and Ras activity with BTA-EG<sub>4</sub> treatment correlate with the age-specific increases in dendritic spine density in a mouse model of AD.

#### BTA-EG<sub>4</sub> improves learning and memory in 3xTg AD mice

To examine whether BTA-EG<sub>4</sub> can improve learning and memory in a mouse model of AD, we injected 2–3 month old, 6–10 month old and 13–16 month old 3xTg AD mice daily for 2 weeks with BTA-EG<sub>4</sub> (30 mg/kg) and conducted the Morris Water Maze. We found that there is an age-dependent progressive loss in the effectiveness of BTA-EG<sub>4</sub> in improving learning and memory of 3xTg AD mice. As seen in Figs. 5A–D, 2–3 month old BTA-EG<sub>4</sub> injected mice demonstrated significantly faster escape latency during training trials and performed

**Fig. 1.** BTA-EG<sub>4</sub> increases dendritic spine density in 3xTg AD mice. (A–E) Representative Golgi-stained dendritic segments of cortical layer II/III pyramidal neurons from 6–10 months of age (A) or 13–16 months of age (B) 3xTg AD mice treated with BTA-EG<sub>4</sub> (“B”) or vehicle (“C”) control. Quantification of averaged spine densities on apical oblique (AO) (C), basal (BS) (D), and total (AO + BS) (E) dendrites ( $n = 4–5$  brains/group; \*\* $p < 0.01$ , \*\*\* $p < 0.001$ ). (F–J) Representative Golgi-stained dendritic segments of cortical layer II/III pyramidal neurons from 6 to 10 months of age (F) or 13–16 months of age (G) 3xTg AD mice treated with BTA-EG<sub>4</sub> or vehicle control. Quantification of averaged spine densities on apical oblique (AO, H), basal (BS, I), and total (AO + BS, J) dendrites ( $n = 3$  brains/group; \*\* $p < 0.01$ , \*\*\* $p < 0.001$ ).

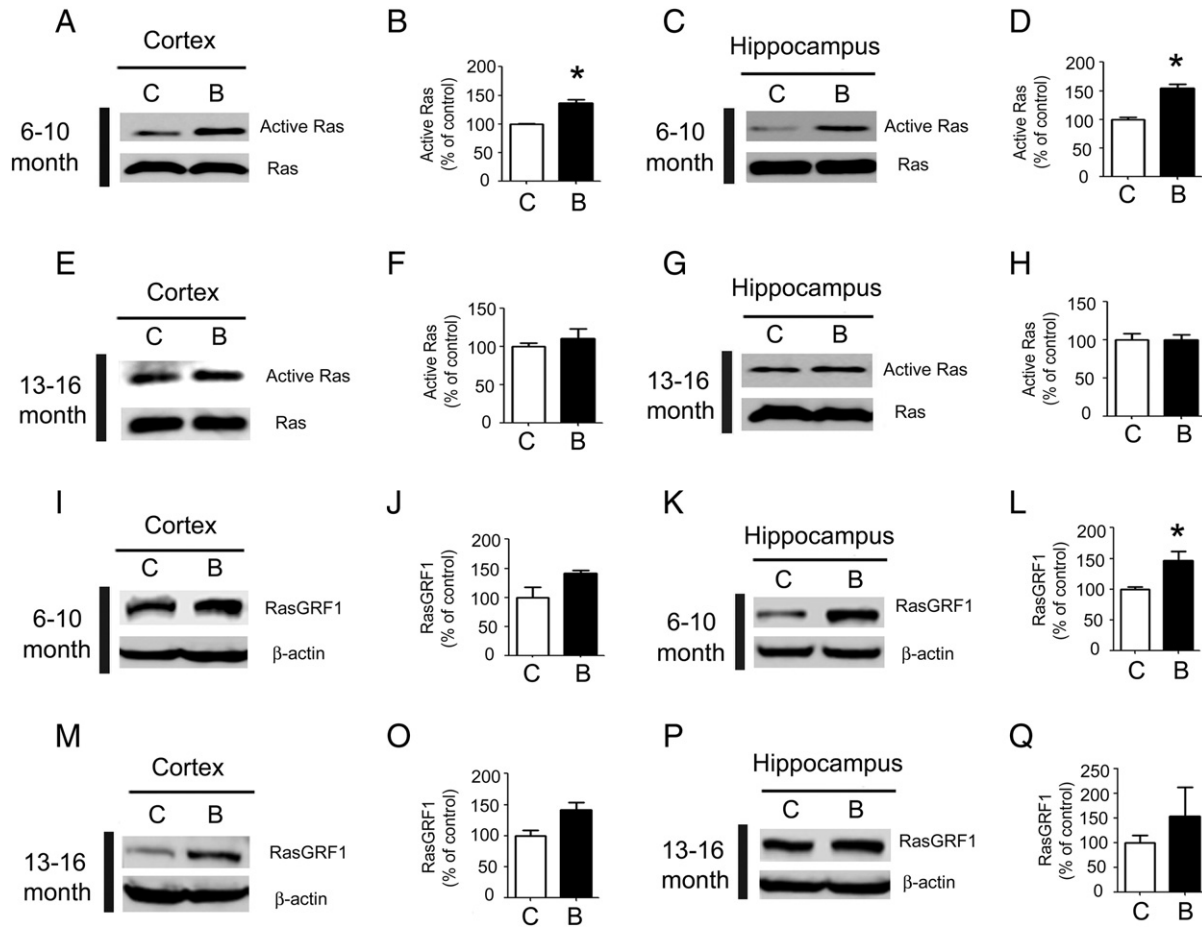


**Fig. 3.** BTA-EG<sub>4</sub> increases Ras activity and RasGRF1 levels in 6–10 month old 3xTg AD mice. GST-Raf1-RBD pull-down of active Ras from brain lysates of cortex and hippocampus from 6–10 month old (A–D) and 13–16 month old (E–H) 3xTg AD mice injected with control or BTA-EG<sub>4</sub> (n = 2 brains/group); \*p < 0.05. (I–L) Western blot of RasGRF1 in brain lysates from cortex (I, J) and hippocampus (K, L) from 6 to 10 month old 3xTg AD mice i.p. injected with vehicle control (“C”) or BTA-EG<sub>4</sub> (“B”) (n = 3–4 brains/group). (M–Q) Western blot of RasGRF1 from cortex (M, O) and hippocampus (P, Q) from 13 to 16 month old 3xTg AD mice injected with BTA-EG<sub>4</sub> or vehicle (n = 3–4 brains/group). β-Actin is used as a loading control; \*p < 0.05.

significantly better during probe trials, as seen by a greater percentage of time in the target quadrant and more platform crossings than control injected mice, without differing in swim speed (Figs. 5A–D, n = 7/

group). This behavioral improvement corresponds to a decrease in soluble Aβ 40 levels following BTA-EG<sub>4</sub> injection in 2–3 month old 3xTg AD mice (Fig. 5M, n = 7/group). At 6–10 months of age, BTA-EG<sub>4</sub>

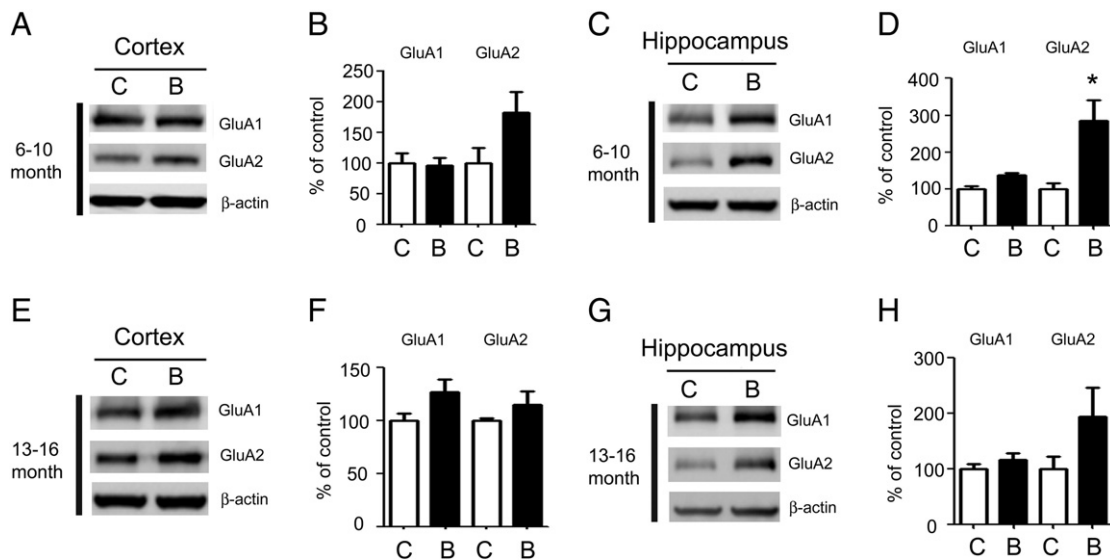


**Fig. 4.** BTA-EG<sub>4</sub> injected mice had increased AMPA receptor subunit GluA2 expression at 6–10 months of age. (A–D) Western blot of GluA1 and GluA2 levels in brain lysates from cortex (A, B) and hippocampus (C, D) of 6–10 month old 3xTg AD mice injected with BTA-EG<sub>4</sub> (“B”) or control vehicle solution (“C”) daily for 2 weeks (n = 3–4 brains/group). (E–H) Western blot of levels of GluA1 and GluA2 in brain lysates from cortex (E, F) and hippocampus (G, H) of 13–16 month old 3xTg AD mice i.p. injected with BTA-EG<sub>4</sub> (“B”) or control (“C”) (n = 3–4 brains/group).

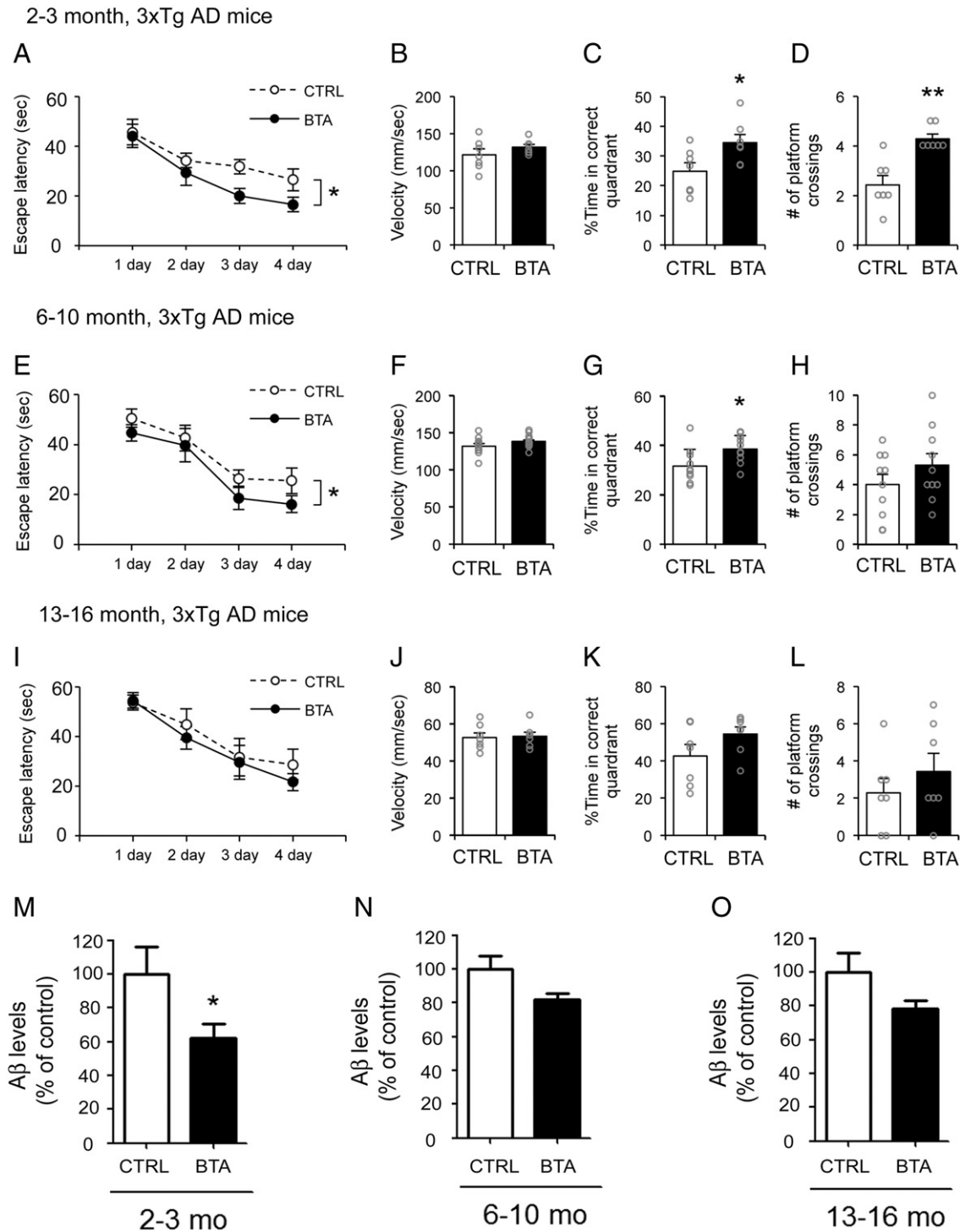


**Fig. 5.** BTA-EG<sub>4</sub> improves cognitive performance of 3xTg AD mice. Spatial learning was tested by Morris Water Maze in 3xTg mice aged 2–3 months ( $n = 7$ /group), 6–10 months ( $n = 10$ /group), and 13–16 months ( $n = 7$ /group). Escape latencies during the 4-day training phase (A, E, I), swim speed velocity during the training trials (B, F, J), percent time spent in the target quadrant measured during the probe test on day 5 (C, G, K), and the number of platform crossings during probe trial on day 5 (D, H, L) were compared between vehicle (CTRL) and BTA-EG<sub>4</sub> (BTA) treated 2–3 month old (A–D), 6–10 month old (E–H), and 13–16 month old (I–L) 3xTg AD mice (\* $p < 0.05$ , \*\* $p < 0.01$ ). A $\beta$  ELISA was conducted to compare A $\beta$  levels in 2–3 month old (M,  $n = 7$ /group), 6–10 month old (N,  $n = 9$ /group), and 13–16 month old (O,  $n = 4$ –5/group) 3xTg AD mice injected with BTA-EG<sub>4</sub> or vehicle daily for 2 weeks.

injected mice still demonstrated faster escape latency during training trials; however, during probe trials, only the percentage of time spent in the target quadrant was significantly improved without changes in the number of platform crossings (Figs. 5E–H,  $n = 10$ /group) or soluble A $\beta$  40 level (Fig. 5N,  $n = 9$ /group). By 13–16 months of age, none of the measured parameters were significantly altered in BTA-EG<sub>4</sub> injected mice (Figs. 5I–L,  $n = 7$ /group, Fig. 5O,  $n = 4$ –5/group). These data suggest that BTA-EG<sub>4</sub> improves both learning and memory on this standard

spatial memory task, but the effectiveness of this drug is limited in older 3xTg AD mice.

## Discussion

This study demonstrates that BTA-EG<sub>4</sub> produces an age-specific improvement in synaptic density and cognitive function in a well-established AD mouse model. In particular, we observed improvement

in dendritic spine density accompanied by changes in dendritic spine morphology in cortical layers II/III and the CA1 region of the hippocampus in 3xTg AD mice. Moreover, BTA-EG<sub>4</sub> increased Ras signaling and subsequent downstream signaling to synaptic AMPA receptors without altering phosphorylation of ERK and Elk in this mouse model, which was also most effective in young animals. Furthermore, we report that BTA-EG<sub>4</sub> is effective at improving memory-related cognitive function. However, the BTA-EG<sub>4</sub>-induced improvement of synaptic loss and cognitive decline in the 3xTg AD mice was most effective at ages before severe synapse loss.

In the present study, we selected a dosage of 30 mg/kg of BTA-EG<sub>4</sub> daily for 2 weeks due to its pronounced effect on dendritic spine density in wild-type mice (Megill et al., 2013). We found that dendritic spine density was increased in both the hippocampus CA1 region and cortical layers II/III at 6–10 months of age (mild A $\beta$  plaque deposition and synapse loss) following BTA-EG<sub>4</sub> treatment in 3xTg AD mice. While BTA-EG<sub>4</sub> was able to ameliorate dendritic spine loss typically seen in 13–16 month old (moderate A $\beta$  plaque deposition and synapse loss) 3xTg AD mice in cortical layers II/III, there was only a trend toward an increase in hippocampal spine density measured in CA1. This suggests that BTA-EG<sub>4</sub> may be useful for improving early AD pathology. However, this limited effect may be due to the short (2-week) duration of BTA-EG<sub>4</sub> treatment; hence, it is possible that a longer treatment period or initiation of the treatment before severe A $\beta$  plaque pathology may be more effective at improving dendritic spine density. Unexpectedly, we also found that dendritic spine density in 6–10 month old 3xTg AD mice is *higher* than that of 2–3 month old 3xTg AD mice. This might be due to either the normal function of APP before amyloid beta deposition that increases dendritic spine number, or the effect of tau increasing dendritic spine density on its own. Another possibility is that this may reflect normal development of dendritic spine density change, which is preserved in the 3xTg AD mice. Future studies are warranted to examine these possibilities. Additionally, it will be of interest to investigate whether BTA-EG<sub>4</sub> has the same effect on dendritic spine density in other mouse models of AD, such as 2xTg AD mice lacking tau pathology. Determining the effectiveness of BTA-EG<sub>4</sub> with and without tau pathology will be informative, especially in light of a recent study demonstrating that tau increases dendritic spine density while tau mutants have reduced dendritic spine density (Kremer et al., 2011).

In addition to dendritic spine density, dendritic spine morphology analyses can elucidate the effects of treatment on synapse formation. For example, long and thin dendritic spines are often classified as “immature learning” spines, whereas short and wide dendritic spines are classified as “mature memory” spines (Kasai et al., 2002; Yasumatsu et al., 2008). Specifically, longer spines are thought of as substrates for conversion into mature spines via LTP-type mechanisms, while wider spines typically mediate stronger synaptic transmission (Matsuzaki et al., 2001). Previously, we reported that BTA-EG<sub>4</sub> injection does not alter dendritic spine morphology in wild-type mice (Megill et al., 2013). Yet, here we observed that BTA-EG<sub>4</sub> alters dendritic spine morphology in 3xTg AD mice at 6–10 months of age. In particular, dendritic spines were longer and wider following daily BTA-EG<sub>4</sub> application for 2 weeks, suggesting that BTA-EG<sub>4</sub> can regulate dendritic spine structure. However, this effect was restricted in age, and we did not observe alterations in dendritic spine morphology in 13–16 month old 3xTg AD mice following BTA-EG<sub>4</sub> treatment. This further corroborates the idea that BTA-EG<sub>4</sub> may be effective at altering dendritic spine morphology before high A $\beta$  plaque load in this AD mouse model. Alternatively, a longer duration of treatment may be needed for altering dendritic spine morphology in aged AD mice with heavier plaque load. AD patients and mouse models of AD undergo decreased synaptic connectivity and increased synaptic loss with age (Knobloch and Mansuy, 2008; Scheff and Price, 2006). Because 13–16 month old 3xTg AD mice have a greater loss of synapses than 6–10 month old mice, it may be more difficult to improve synapse number with only 2 weeks of BTA-EG<sub>4</sub> treatment.

We recently demonstrated that BTA-EG<sub>4</sub> promotes dendritic spine density through a full length APP and Ras-dependent mechanism in wild-type mice (Megill et al., 2013). Additionally, a recent study demonstrates that A $\beta$  (in contrast to the effect of full length APP) decreases dendritic spine density by inhibiting Ras activity (Szatmari et al., 2013). Here, we found that Ras activity is increased following BTA-EG<sub>4</sub> injection in 6–10 month old, but not 13–16 month old, 3xTg AD mice. We also found that BTA-EG<sub>4</sub> can selectively increase GluA2 levels while GluA1 levels remained comparable to controls. It is known that Ras activity can regulate AMPA receptor expression (Gu and Stornetta, 2007; Qin et al., 2005), and in particular GluA2 subunit expression has been shown to increase dendritic spine density via its extracellular domain (Passafaro et al., 2003). Surprisingly, BTA-EG<sub>4</sub> injections in 6–10 month old 3xTg AD mice did not alter downstream targets of Ras, such as p-ERK and p-Elk. This is opposite to the effects of BTA-EG<sub>4</sub> in wild-type mice in which downstream Ras targets were increased. This discrepancy may be explained by the complexities of Ras signaling in various circumstances, including localization of Ras isoforms and the disease state of the organism. It is known that Ras activates ERK in an isoform-specific manner (Prior and Hancock, 2012), and thus, BTA-EG<sub>4</sub> may act differentially to promote dendritic spine density in wild-type mice (the normal condition) and in a mouse model of AD (the pathological condition). One possibility may be that BTA-EG<sub>4</sub> upregulates an isoform of Ras through RasGRF1 that poorly activates ERK (and its downstream target Elk) in 3xTg AD mice, as opposed to the effects of BTA-EG<sub>4</sub> in wild-type mice (to increase both Ras and ERK). One candidate Ras isoform activated by RasGRF1 is localized to the endoplasmic reticulum and has been shown to activate ERK less efficiently than other Ras isoforms (Matallanas et al., 2006). Thus, this isoform may be capable of regulating glutamate receptor insertion at the synapse in a manner that does not rely on ERK upregulation in 3xTg mice. In any case, it is likely that BTA-EG<sub>4</sub> promotes dendritic spine density through enhancing Ras activity and increasing GluA2 AMPA receptor subunit expression in 3xTg AD mice. Alternatively, BTA-EG<sub>4</sub> may also exert its effect by neutralizing A $\beta$ , which has been shown to induce removal of synaptic AMPARs and reduce the density of dendritic spines (Hsieh et al., 2006; Kamenetz et al., 2003). These two possibilities are not mutually exclusive, and it is possible that the combination of increasing Ras signaling and blocking A $\beta$  signaling may be responsible for the improvement in dendritic spine density in 3xTg AD mice with BTA-EG<sub>4</sub> treatment.

We further found that BTA-EG<sub>4</sub> improves learning and memory in 3xTg AD mice. This effect is similar to what we observed in wild-type mice (Megill et al., 2013), but with subtle differences. In wild-type mice, BTA-EG<sub>4</sub> mainly improved memory with little improvement on learning (Megill et al., 2013). However, in 3xTg AD mice, both learning and memory are improved by BTA-EG<sub>4</sub>. In particular, this improvement was only significant in the 2–3 month old and 6–10 month old, but not in the 13–16 month old, 3xTg AD mice. We further found that BTA-EG<sub>4</sub> improved cognitive performance that correlated with decreased Soluble A $\beta$  40 levels in 2–3 month old 3xTg AD mice, along with a trend toward a decrease at 6–10 months and 13–16 months of age. The age dependence of the effectiveness of BTA-EG<sub>4</sub> mirrors that seen with dendritic spine improvement and Ras signaling. As discussed above, it would be of interest to investigate whether a longer treatment period or initiation of the treatment before A $\beta$  plaque accumulation could be more effective at recovering behavioral performance. In either case, our current data strongly suggest that BTA-EG<sub>4</sub> treatment may be useful for the prevention of early AD pathology.

## Conclusions

Our study demonstrates that BTA-EG<sub>4</sub> treatment can increase dendritic spine density in a mouse model of AD with mild and moderate A $\beta$  plaque deposition and synapse loss. This change in dendritic spine

density was associated with increased Ras activity. Moreover, we observed that BTA-EG<sub>4</sub> injected mice show improvement in learning and memory up to 6–10 months of age. Taken together, these findings suggest that BTA-EG<sub>4</sub> may be a beneficial therapy for preventing and/or treating the synaptic loss accompanying AD.

Supplementary data to this article can be found online at <http://dx.doi.org/10.1016/j.expneurol.2013.11.023>.

## Acknowledgments

This work was supported by the National Institutes of Health (NIH) Grant AG039708 (HSH) and NIH AG044339 (HSH), and the UCSD Alzheimer's Disease Research Center NIH 3P50 AG005131 (JY).

## References

- Capule, C.C., Yang, J., 2012. Enzyme-linked immunosorbent assay-based method to quantify the association of small molecules with aggregated amyloid peptides. *Anal. Chem.* 84, 1786–1791.
- Finder, V.H., Glockshuber, R., 2007. Amyloid-beta aggregation. *Neurodegener. Dis.* 4, 13–27.
- Gu, Y., Stornetta, R.L., 2007. Synaptic plasticity, AMPA-R trafficking, and Ras-MAPK signaling. *Acta Pharmacol. Sin.* 28, 928–936.
- Habib, L.K., Lee, M.T., Yang, J., 2010. Inhibitors of catalase-amyloid interactions protect cells from beta-amyloid-induced oxidative stress and toxicity. *J. Biol. Chem.* 285, 38933–38943.
- Hsieh, H., Boehm, J., Sato, C., Iwatsubo, T., Tomita, T., Sisodia, S., Malinow, R., 2006. AMPAR removal underlies Abeta-induced synaptic depression and dendritic spine loss. *Neuron* 52, 831–843.
- Inbar, P., Li, C.Q., Takayama, S.A., Bautista, M.R., Yang, J., 2006. Oligo(ethylene glycol) derivatives of thioflavin T as inhibitors of protein-amyloid interactions. *Chembiochem* 7, 1563–1566.
- Kamenetz, F., Tomita, T., Hsieh, H., Seabrook, G., Borchelt, D., Iwatsubo, T., Sisodia, S., Malinow, R., 2003. APP processing and synaptic function. *Neuron* 37, 925–937.
- Kasai, H., Matsuzaki, M., Noguchi, J., Yasumatsu, N., 2002. Dendritic spine structures and functions. *Nihon Shinkai Seishin Yakurigaku Zasshi* 22, 159–164.
- Knobloch, M., Mansuy, I.M., 2008. Dendritic spine loss and synaptic alterations in Alzheimer's disease. *Mol. Neurobiol.* 37, 73–82.
- Kremer, A., Maurin, H., Demedts, D., Devijver, H., Borghgraef, P., Van Leuven, F., 2011. Early improved and late defective cognition is reflected by dendritic spines in Tau.P301L mice. *J. Neurosci.* 31, 18036–18047.
- Lustbader, J.W., Cirilli, M., Lin, C., Xu, H.W., Takuma, K., Wang, N., Caspersen, C., Chen, X., Pollak, S., Chaney, M., Trinchese, F., Liu, S., Gunn-Moore, F., Lue, L.F., Walker, D.G., Kuppasamy, P., Zewier, Z.L., Arancio, O., Stern, D., Yan, S.S., Wu, H., 2004. ABAD directly links Abeta to mitochondrial toxicity in Alzheimer's disease. *Science* 304, 448–452.
- Masliyah, E., Crews, L., Hansen, L., 2006. Synaptic remodeling during aging and in Alzheimer's disease. *J. Alzheimers Dis.* 9, 91–99.
- Matallanas, D., Sanz-Moreno, V., Arozarena, I., Calvo, F., Agudo-Ibanez, L., Santos, E., Berciano, M.T., Crespo, P., 2006. Distinct utilization of effectors and biological outcomes resulting from site-specific Ras activation: Ras functions in lipid rafts and Golgi complex are dispensable for proliferation and transformation. *Mol. Cell Biol.* 26, 100–116.
- Matsuzaki, M., Ellis-Davies, G.C., Nemoto, T., Miyashita, Y., Iino, M., Kasai, H., 2001. Dendritic spine geometry is critical for AMPA receptor expression in hippocampal CA1 pyramidal neurons. *Nat. Neurosci.* 4, 1086–1092.
- Megill, A., Lee, T., Dibattista, A.M., Song, J.M., Spitzer, M.H., Rubinshtein, M., Habib, L.K., Capule, C.C., Mayer, M., Turner, R.S., Kirkwood, A., Yang, J., Pak, D.T., Lee, H.K., Hoe, H.S., 2013. A tetra(ethylene glycol) derivative of benzothiazole aniline enhances Ras-mediated spinogenesis. *J. Neurosci.* 33, 9306–9318.
- Minami, S.S., Clifford, T.G., Hoe, H.S., Matsuoka, Y., Rebeck, G.W., 2012. Fyn knock-down increases Abeta, decreases phospho-tau, and worsens spatial learning in 3xTg-AD mice. *Neurobiol. Aging* 33 (4), 825.e15–24.
- Oddo, S., Caccamo, A., Shepherd, J.D., Murphy, M.P., Golde, T.E., Kaye, R., Metherate, R., Mattson, M.P., Akbari, Y., LaFerla, F.M., 2003. Triple-transgenic model of Alzheimer's disease with plaques and tangles: intracellular Abeta and synaptic dysfunction. *Neuron* 39, 409–421.
- Passafium, M., Nakagawa, T., Sala, C., Sheng, M., 2003. Induction of dendritic spines by an extracellular domain of AMPA receptor subunit GluR2. *Nature* 424, 677–681.
- Prior, I.A., Hancock, J.F., 2012. Ras trafficking, localization and compartmentalized signaling. *Semin. Cell Dev. Biol.* 23, 145–153.
- Qin, Y., Zhu, Y., Baumgart, J.P., Stornetta, R.L., Seidenman, K., Mack, V., van Aelst, L., Zhu, J.J., 2005. State-dependent Ras signaling and AMPA receptor trafficking. *Genes Dev.* 19, 2000–2015.
- Scheff, S.W., Price, D.A., 2006. Alzheimer's disease-related alterations in synaptic density: neocortex and hippocampus. *J. Alzheimers Dis.* 9, 101–115.
- Scheff, S.W., Price, D.A., Schmitt, F.A., Mufson, E.J., 2006. Hippocampal synaptic loss in early Alzheimer's disease and mild cognitive impairment. *Neurobiol. Aging* 27, 1372–1384.
- Scheff, S.W., Price, D.A., Schmitt, F.A., DeKosky, S.T., Mufson, E.J., 2007. Synaptic alterations in CA1 in mild Alzheimer disease and mild cognitive impairment. *Neurology* 68, 1501–1508.
- Selkoe, D.J., 2002. Alzheimer's disease is a synaptic failure. *Science* 298, 789–791.
- Szatmari, E.M., Oliveira, A.F., Sumner, E.J., Yasuda, R., 2013. Centaurin-alpha1-Ras-Elk-1 signaling at mitochondria mediates beta-amyloid-induced synaptic dysfunction. *J. Neurosci.* 33, 5367–5374.
- Terry, R.D., Masliyah, E., Salmon, D.P., Butters, N., DeTeresa, R., Hill, R., Hansen, L.A., Katzman, R., 1991. Physical basis of cognitive alterations in Alzheimer's disease: synapse loss is the major correlate of cognitive impairment. *Ann. Neurol.* 30, 572–580.
- Yasumatsu, N., Matsuzaki, M., Miyazaki, T., Noguchi, J., Kasai, H., 2008. Principles of long-term dynamics of dendritic spines. *J. Neurosci.* 28, 13592–13608.